Arctic surface temperature change to emissions of black carbon within Arctic or midlatitudes

Maria Sand,[1] Terje Koren Berntsen,[1] Øyvind Seland,[2] and Jón Egill Kristjánsson[1]

Received 4 April 2013; revised 28 June 2013; accepted 28 June 2013; published 30 July 2013.

[1] In this study, we address the question of how sensitive the Arctic climate is to black carbon (BC) emitted within the Arctic compared to BC emitted at midlatitudes. We consider the emission-climate response spectrum and present a set of experiments using a global climate model. A new emission data set including BC emissions from flaring and a seasonal variation in the domestic sector has been used. The climate model includes a snow model to simulate the climate effect of BC deposited on snow. We find that BC emitted within the Arctic has an almost five times larger Arctic surface temperature response (per unit of emitted mass) compared to emissions at midlatitudes. Especially during winter, BC emitted in North-Eurasia is transported into the high Arctic at low altitudes. A large fraction of the surface temperature response from BC is due to increased absorption when BC is deposited on snow and sea ice with associated feedbacks. Today there are few within-Arctic sources of BC, but the emissions are expected to grow due to increased human activity in the Arctic. There is a great need to improve cleaner technologies if further development is to take place in the Arctic, especially since the Arctic has a significantly higher sensitivity to BC emitted within the Arctic compared to BC emitted at midlatitudes.

Citation: Sand, M., T. K. Berntsen, Ø. Seland, and J. E. Kristjánsson (2013), Arctic surface temperature change to emissions of black carbon within Arctic or midlatitudes, *J. Geophys. Res. Atmos.*, *118*, 7788–7798, doi:10.1002/jgrd.50613.

1. Introduction

[2] The Arctic has warmed rapidly over the last century with a rate almost twice as fast as the global mean rate [*Intergovernmental Panel on Climate Change*, 2007]. The temperature increase is accompanied by an earlier spring melt and a lengthening of the melting season, a decrease in the sea-ice extent, and a thinning of the Greenland ice sheet [*AMAP*, 2011, 2012]. Studies show an Arctic amplification to global emissions of black carbon (BC), which absorbs solar radiation in the atmosphere and when deposited on snow [e.g., *Hansen and Nazarenko*, 2004; *Jacobson*, 2004; *Flanner et al*., 2007; *Koch et al*., 2009a]. Reduction of BC emissions has been suggested as a short-term climate control strategy [*Hansen et al*., 2000; *Quinn et al*., 2008; *Jacobson*, 2010; *Shindell et al*., 2012]. Several studies have identified the different sources of BC reaching the Arctic and the impact of BC in the Arctic in terms of radiative forcing (per unit emission) [*Koch and Hansen*, 2005; *Stohl*, 2006]. Other studies have calculated the Arctic climate response to local and remote BC forcing [*Shindell*, 2007; *Koch et al*., 2011a]. For absorbing aerosols, such as BC, there is no simple relationship between the forcing and the response in the Arctic [*Hansen et al*., 2005]. In order to establish meaningful mitigation actions for BC, it is necessary to consider the entire emission-climate response spectrum to estimate which emissions contribute to Arctic warming.

[3] Unlike scattering aerosols that exert a weak (negative) forcing over snow, BC aerosols absorb solar radiation and exert a positive forcing over white surfaces, both in the atmosphere and when deposited on snow. This makes the forcing and the potential impact of BC particularly high in the Arctic during spring, when there are large amounts of sunlight available, most of the surfaces are still covered with snow and sea ice, and the BC concentrations are at a maximum [*Hansen and Nazarenko*, 2004; *Flanner et al*., 2009]. Arctic BC originates mostly from source areas outside the Arctic and is a result of a long-range transport from lower latitudes [*Law and Stohl*, 2007]. In the Arctic boundary layer, surfaces of low potential temperatures form a dome over the Arctic [*Klonecki et al*., 2003]. The high static stability associated with strong surface inversions in the Arctic boundary layer suppresses the mixing of pollution and heat from the free troposphere to the boundary layer, and BC reaching the Arctic from lower latitudes is not easily deposited on the Arctic surface. Several model studies highlight the importance of the vertical distribution of BC in regards to the climate response [*Hansen et al*., 2005; *Ban-Weiss et al*., 2012; *Flanner*, 2013; *Samset et al*., 2013]. *Flanner* [2013] perturbed BC mass in different altitudes in the Arctic and found a strong surface warming for BC located

[1]Department of Geosciences, University of Oslo, Oslo, Norway.
[2]Norwegian Meteorological Institute, Oslo, Norway.

Corresponding author: M. Sand, Department of Geosciences, P.O. Box 1022, 0315 Oslo, Norway. (maria.sand@geo.uio.no)

2169-897X/13/10.1002/jgrd.50613

near the surface, a weak surface warming for BC at 400−750 hPa, and a surface cooling for BC at 210–250 hPa. An earlier study showed similar trends in the sign of temperature change for BC perturbations at the global scale [*Ban-Weiss et al*., 2012]. Previous studies have shown that atmospheric absorption by present-day BC in the Arctic atmosphere (i.e., neglecting the impact of surface deposition) may have a small or even negative impact on the surface temperatures, as most of the BC aerosols are located above the Arctic dome [*Shindell and Faluvegi*, 2009; *Sand et al*., 2013]. The studies indicate the mitigation strategies for present-day BC should target emissions outside the Arctic. However, potential BC sources within the Arctic dome are more likely to warm the surface due to the near surface solar heating and the greater likelihood of surface deposition. The boundaries of the Arctic dome are highly variable in time and space, with a maximum extension over Eurasia during winter. Here the snow-covered surfaces make the air sufficiently cold, so that pollution can be transported directly into the high-Arctic boundary layer [*Stohl*, 2006]. Emissions during winter in Eurasia will therefore have a greater impact on the Arctic climate, highlighting the importance of seasonal differences in emissions.

[4] Current inventory estimates show that the dominant BC emissions within the Arctic today are caused by flaring related to the oil and gas fields in North Western Russia [*Stohl et al*., 2013]. Compared to midlatitudes, within-Arctic BC emissions are low, but the emissions are expected to grow due to new developments in the Arctic, the opening of the Northern sea routes to shipping, and enhanced oil and gas exploration [*Corbett et al*., 2010; *Peters et al*., 2011; *Ødemark et al*., 2012]. The use of wood stoves in the Nordic countries, Russia, Canada and Alaska during winter is one example of emissions in the domestic sector that have a large impact per unit emission in the Arctic. These emissions are expected to increase [*AMAP*, 2011, 2012].

[5] As the model studies of *Shindell and Faluvegi* [2009], *Sand et al*. [2013] and *Flanner* [2013] focused on the local climate response to local BC forcing, the studies are less relevant for policies that focus on mitigation of BC emissions at high latitudes. In this study, we want to study the climate effect of emitting BC in different regions. We investigate how anthropogenic BC emissions within-Arctic or from midlatitudes influence the Arctic climate, both through absorption in the atmosphere and through changes in surface albedo when BC is deposited on snow and sea ice. The scientific questions we want to address are: (1) How different will the Arctic climate response to BC emissions be if BC is emitted within the Arctic, compared to if BC is transported from lower latitudes and (2) how much of the BC forcing and response in the Arctic can be attributed to BC deposited on snow and sea ice? Since BC perturbs the climate system in many ways, both directly and indirectly, we have performed climate experiments with a global climate model, together with a snow model to include the effects of BC deposition on snow. A new emission data set has been used for BC that includes BC emissions from flaring, and a seasonal variation in the domestic sector, to account for amplified use of wood stoves during the cold season [*Klimont et al*., 2013].

2. Methods

[6] The experiments in this study have been performed with the Norwegian Earth System Model (NorESM) [*Bentsen et al*., 2013; *Iversen et al*., 2013], largely based on the NCAR CCSM4.0 [*Gent et al*., 2011]. The atmospheric model CAM4 [*Neale et al*., 2010] has been modified to include an aerosol module with separate representation of aerosols, aerosol-radiation, and aerosol-cloud interactions with prognostic cloud droplet number concentration [*Kirkevåg et al*., 2013]. The ocean model is replaced by the MICOM model. A snow model, SNICAR [*Flanner and Zender*, 2005], is applied to calculate the snow/albedo TOA RF from BC in snow on land. The sea-ice and the land models are the same as CCSM4.0 and NCAR CESM1.0, respectively, except that the albedo effects of BC and mineral dust aerosols deposited on snow and sea ice are based on the aerosol calculations in CAM4-Oslo. The sea-ice component is based on version 4 of the Los Alamos National Laboratory sea-ice model (CICE4) as described by *Hunke and Lipscomb* [2008]. The sea ice is deformed and transported in response to the ocean currents and wind field. NorESM has been validated against observations in *Bentsen et al*. [2013].

[7] The aerosol module calculates concentrations of aerosols that are tagged according to production mechanisms and size modes. For each of the mass concentrations, there are up to four size modes (nucleation, aitken, accumulation, and coarse). The production mechanisms are gaseous and aqueous chemical production, gas-to-particle nucleation, condensation on aerosol surfaces, and coagulation of smaller particles onto Aiken, accumulation, and coarse mode particles. The tagged information is transported along with the species. The aerosol life-cycle scheme includes sulphate, BC, organic matter (OM), sea-salt, and mineral dust, in addition to the precursors, SO_2 and DMS. There are 11 components for externally mixed particles that are calculated in the life-cycle scheme (and transported in the model). In addition, there are nine components that are tagged according to production mechanisms in air or clouds droplets. The size-resolved transformations into internal mixture with the 11 components can then be estimated a posteriori by use of look-up tables. Aerosol optical properties and CCN calculations are tabulated for a large number of entry values of the process-tagged concentrations, relative humidity, and supersaturation. Hygroscopic swelling is treated by use of the Köhler equation, and optical properties are estimated from Mie theory. CCN activation is estimated based on supersaturations calculated from Köhler theory. The direct effect of aerosols and both the first and second indirect effects are calculated based on a double-moment liquid microphysical scheme [*Storelvmo et al*., 2006]. The only second indirect effect calculated in the model is the autoconversion of liquid cloud water to rain in warm clouds [*Kristjánsson*, 2002]. The indirect effects associated with ice- and mixed-phase clouds are not calculated. The aerosol module, including the parameterization of optical properties and CCN activation, is described in more detail in *Kirkevåg et al*. [2013].

[8] Globally averaged, almost 40% of BC in the model is emitted from fossil fuel combustion. Most of fossil fuel BC is emitted in the nucleation mode, and 10% is assumed

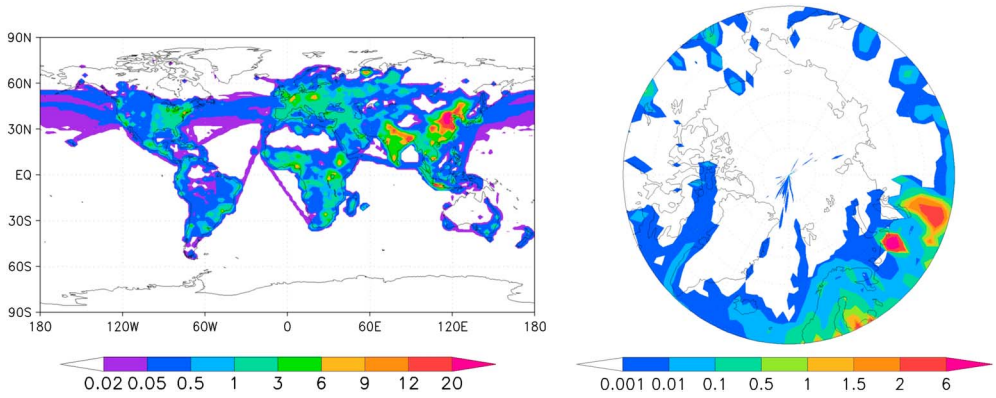

Figure 1. The combined annual mean fossil fuel and biofuel BC emissions for the year 2008 from the reference run. The right figure shows the same quantity within-Arctic only (60–90°N). All units in ng m^{-2} s^{-1}.

emitted as agglomerated BC in the accumulation mode. Emitted fossil fuel BC and OM are assumed externally mixed, while emitted biomass BC and OM are assumed internally mixed. Externally mixed BC is fully hydrophobic. Once emitted, BC gradually turns into hydrophilic, internally mixed aerosols when gaseous sulphate condenses on the particles or by coagulation with sulphate or sea salt. BC is removed from the atmosphere both by dry and wet deposition, although wet deposition dominates the total numbers. The dry deposition velocity depends on particle size, and the relative humidity influences this dependence for hygroscopic particles. Wet deposition is parameterized with an in-cloud scavenging coefficient defined as the mass fraction of the aerosol mode within the cloud droplet. The rainout is then determined by the local precipitation production rate for liquid water.

[9] The 2008 emission inventory that is used for BC fossil fuel and biofuel is from the ECLIPSE project [*Kupiainen and Klimont*, 2007; *Klimont et al*., 2009; *Shindell et al*., 2012; *Klimont et al*., 2013] available through the project website (http://eclipse.nilu.no). All other emissions inventories are from IPCC [*Lamarque et al*., 2010]. In the ECLIPSE inventory, the BC domestic sector has a seasonal variation with a wintertime maximum, and the emissions from flaring are included. The BC emissions from shipping are from the IPCC, as they were not available in ECLIPSE. Emissions from aircrafts are not included as we wanted to focus on ground-based emissions. As the current version of NorESM does not treat the influence of BC on ice nucleation, the impact of aircraft emissions in the Arctic would likely be underestimated [*Jacobson et al*., 2012]. Figure 1 shows the annual mean fossil fuel and biofuel BC emissions for year 2008 used in this study. The global annual mean (fossil fuel and biofuel) BC emissions are 5.5 Tg yr^{-1}. Averaged over the Arctic (60–90°N) and mid-latitudes (28–60°N) only, the emissions are 0.07 Tg yr^{-1} and 2.6 Tg yr^{-1}, respectively.

[10] The model is run on a 1.9° × 2.5° horizontal grid with 26 vertical layers in the atmosphere. The climate simulations have been run for 60 years from a 140 year spin-up with the same 2008 emissions and greenhouse gas levels. The last 30 years have been used for analyses. The climate simulations include one control run, four perturbed runs, and one sensitivity run; six in total. The perturbed runs are: "ARCem" — with BC emissions scaled up north of 60°N, and "MIDem": — with BC emissions scaled up in the midlatitudes (28–60°N). Table 1 shows the annual mean emitted BC mass and column burden for each experiment. The scaling factors were chosen to give regional RF within the Arctic of similar magnitude and to ensure that the results from the climate model were statistically significant. The RF for each experiment is given in Table 2. There is a balance between achieving a statistically significant signal and at the same time limiting nonlinear effects. *Hansen et al*. [2005] found an approximate limit for linearity for scaling giving a global aerosol RF on the order of 1 W m^{-2}. To distinguish the climate impact of BC deposited on snow and sea ice, the two perturbed runs have been repeated without any impact of BC deposited on snow and ice. To further test the Arctic sensitivity to within-Arctic emissions, a highly idealized simulation with identical BC emissions in every Arctic grid cell has been performed (the sensitivity run "gridARC"). The Arctic is defined here as north of 60°N. The instantaneous RF of BC at TOA is estimated in separate five year offline runs with the same experimental setup as the online runs. In the offline runs, the aerosols do not affect the meteorology in the model, so that each simulation has the same meteorology. The snow/albedo RF from BC deposited on snow on land has been calculated with the SNICAR model at each radiative transfer time step as the difference in absorption with and without BC. In the model, BC is deposited both on snow on land and on the sea ice, and change the surface albedo. We lack, however, the instantaneous RF diagnose output for the RF of BC deposited in the sea-ice model. Therefore, the snow/albedo RF reported in this study is for BC deposited on snow on land only. The full climate response in the coupled runs includes the snow/albedo effect of BC deposited on both snow on land and on the sea ice.

Table 1. Emitted BC Mass and BC Column Burden Averaged in Two Latitude Bands (60–90°N and 28–60°N)

	EMITTED BC MASS[a]		BC COLUMN BURDEN[b]	
	Tg BC $year^{-1}$		mg/m^{-2}	
	60–90°N	28–60°N	60–90°N	28–60°N
ARCem	8.8	0	2.4	0.5
MIDem	0	20.8	1.3	2.5
gridARC	9.2	0	1.8	0.3

[a]Annual mean emitted fossil fuel and biofuel BC mass (perturbed control).
[b]Annual mean increase in BC column burden (perturbed control).

Table 2. Radiative Forcing, Surface Temperature Response, and Climate Sensitivity[a]

	RF TOA[b]			Snow/Alb. RF.[c]			Norm. RF[d]		ΔTs		ΔTs nodep[e]		Sensitivity[f]	
	W m^{-2}			W m^{-2}			W m^{-2} (Tg yr^{-1})$^{-1}$		K		K		K (Tg yr^{-1})$^{-1}$	
	60–90°N	28–60°N	global	60–90°N	28–60°N	global	60–90°N	global	60–90°N	global	60–90°N	global	60–90°N	global
ARCem	2.58	0.58	0.31	1.18	0.08	0.09	0.38	0.04	2.32	0.32	0.74	0.24	0.24	0.03
MIDem	3.11	3.44	1.28	0.48	0.19	0.07	0.17	0.07	0.99	0.30	0.20	0.26	0.05	0.01
gridARC	2.59	0.32	0.25	2.22	0.08	0.16	0.47	0.04	3.91	0.42	-	-	0.38	0.04

[a]The quantities are annual means in the Arctic (60–90°N), in the midlatitudes (28–60°N), and global.
[b]Direct and indirect radiative forcing TOA.
[c]TOA RF from BC deposited on snow on land (not sea ice).
[d]Total RF (direct, indirect and snow/albedo effect from BC on snow on land) per global emission increase.
[e]Surface temperature response without deposition of BC (for the ARCem and MIDem experiments only).
[f]Surface temperature change per global emission increase.

3. Results

3.1. BC Concentrations in the Atmosphere and Snow

[11] Figure 2 shows the annual zonal mean BC concentrations for the reference run. While the maxima in BC concentrations at midlatitudes are near the source areas at the surface, in the Arctic, the maximum BC concentrations are found at around 500 hPa. The annual mean concentration of BC deposited in snow on land for the reference run is shown in Figure 3. The maximum is located near the emission hot spot in China with concentrations above 1200 ng per gram of snow. In Figure 4, the modeled concentrations of BC in snow are compared to observations in the Arctic taken from *Doherty et al*. [2010] and from northwestern China from *Ye et al*. [2012]. Each observation is compared to BC concentration in the top snow layer in the nearest model grid box in the actual month in the reference run. The filled circles represent the average of the observations in the different locations, and the lines represent the maximum and minimum observation. Despite the fact that the observations represent point observations at limited time intervals, the monthly mean modeled concentrations agree reasonably well with the observations. NorESM (with IPCC BC emissions) has been validated against BC observations in *Sand et al*. [2013] and *Kirkevåg et al*. [2013]. Here it was shown that NorESM underestimates global BC surface concentrations by 36% and is unable to reproduce the observed Arctic haze during winter and early spring (while during summer and autumn the concentrations are within the same size order). Using the Eclipse emission inventory, the wintertime surface BC concentrations in the high-Arctic are doubled compared to the emission inventory from the IPCC (which did not include flaring or a seasonal variation in the domestic sector), suggesting that a part of the underestimation in the model is linked to emission data.

[12] Figure 5 shows the increase in the zonal mean BC concentrations during the winter and summer seasons for the two experiments, ARCem and MIDem. In MIDem, the highest perturbation of the BC concentrations is during the winter at 30–40°N. In the winter, some of the BC is transported into the Arctic at low altitudes, but most of the BC is lifted above the boundary layer. During summer, the concentrations in midlatitudes and the Arctic are convectively lifted, leading to an increase in the BC concentrations at high altitudes and a

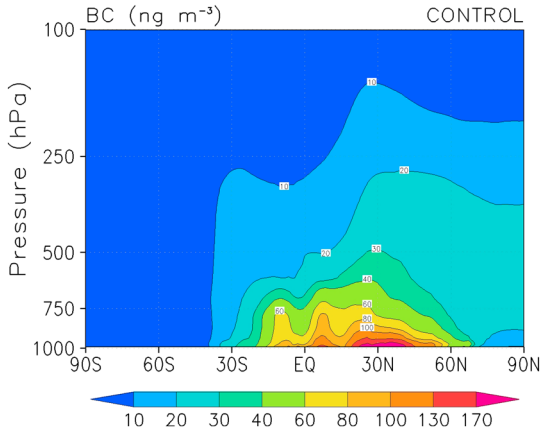

Figure 2. Annual zonal mean BC concentrations (in ng m^{-3}) for the reference run with 2008 emissions.

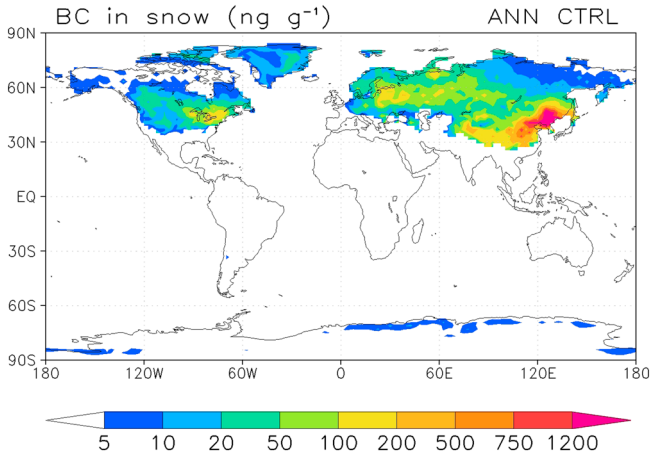

Figure 3. Annual mean BC concentrations in snow on land (in ng BC per g snow) averaged when there is snow present from the reference run with 2008 emissions.

decrease in the concentrations at lower altitudes. For ARCem, there is a larger seasonal difference between the perturbations in the Arctic surface BC concentrations, with a maximum during winter when BC is transported at low altitudes along the cold surface in North-Eurasia into the high-Arctic boundary layer. During summertime, BC perturbations reach the high-Arctic at higher altitudes (900–500 hPa) with a lower enhancement of surface concentrations.

3.2. BC Forcing

[13] The direct and indirect RF of BC in the atmosphere have been calculated as the change in the incoming and outgoing radiation at TOA in the offline runs with and without perturbed BC. Table 2 summarizes the annual mean RF for BC in the atmosphere and RF of the snow/albedo effect on snow on land for the experiments. Following previous studies [*Shindell and Faluvegi*, 2009; *Sand et al.*, 2013], we calculate the RF in latitude bands as well as the global mean. For MIDem, the TOA RF at midlatitudes is 3.4 W m^{-2}. The Arctic TOA RF for MIDem (3.1 W m^{-2}) is higher than for ARCem (2.6 W m^{-2}).

[14] Figure 6 shows the Arctic mean seasonal cycle for the direct and indirect RF of atmospheric BC and the snow/albedo effect for ARCem and MIDem. The direct RF for ARCem and MIDem peaks in the summer season when there is maximum insolation while the snow/albedo effect peaks earlier in the melt season when the snow cover is still extensive. As expected, the Arctic annual mean indirect RF is much smaller than the direct RF: 0.17 W m^{-2} for ARCem and 0.08 W m^{-2} for MIDem [*Koch et al.*, 2011b]. Note that the indirect forcing in NorESM is calculated for liquid clouds only. While the direct RF for the MIDem case is slightly larger than ARCem, the snow/albedo effect for BC in MIDem is smaller (1.2 W m^{-2} for ARCem and 0.48 W m^{-2} for MIDem). Normalizing each case to the increase in emissions the total forcing (direct and indirect RF of atmospheric BC and the snow/albedo effect) per unit emission is twice as large for ARCem as for MIDem (0.38 W m^{-2} per Tg yr^{-1} vs. 0.17 W m^{-2} per Tg yr^{-1}).

3.3. Arctic Climate Response

[15] The changes in the Arctic annual mean atmospheric energy budget for ARCem and MIDem (from the coupled multidecadal climate simulations) are shown in Figure 7. The direct effect of shortwave radiation at TOA due to increased BC absorption is the main driver for both ARCem and MIDem. For ARCem, the snow/albedo effect is also important. The net surface shortwave radiation, which includes increased absorption at the surface and a reduction due to dimming, is about half of that at TOA. The net shortwave flux at the surface increases both due to absorption of BC at the surface and the lowering of the surface albedo when a darker surface is exposed after melting of snow and sea ice. *Shindell and Faluvegi* [2009] and *Sand et al.* [2013] showed that atmospheric BC forcing (with a vertical profile as in their reference simulations) at midlatitudes had a warming effect on the Arctic surface, while BC forcing in the Arctic had a cooling effect. The MIDem experiment in this study can be considered a combination of both forcings (Arctic + midlatitudes), as BC emitted at midlatitudes is transported into Arctic. *Shindell and Faluvegi* [2009] and *Sand et al.* [2013] found that the atmospheric heating at midlatitudes caused an increase in the northward heat transport, while in their Arctic experiment it decreased. We have calculated the northward heat transport as a residual between the energy budget at TOA and at the surface. The change in the northward heat transport for MIDem in this case is negative by −2 W m^{-2}. This indicates that when regional emissions are considered, the effect of BC transported to the Arctic and causing absorption there dominates in the MIDem experiment. Thus, the direction of the northward heat transport perturbation is opposite compared to the response to the concentration perturbations (in latitude bands) studied by *Shindell and Faluvegi* [2009] and *Sand et al.* [2013].

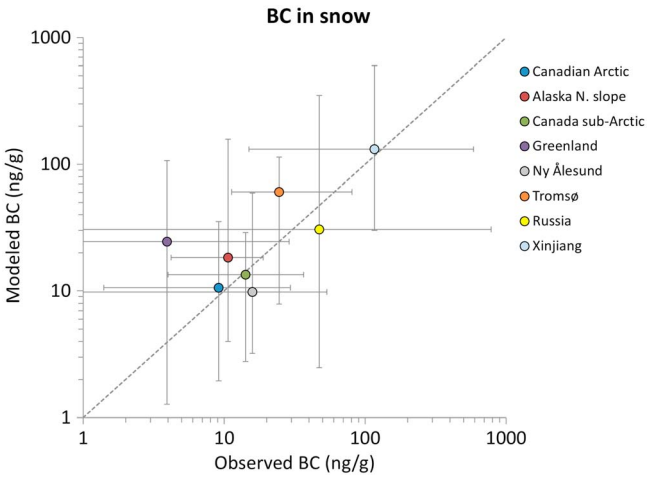

Figure 4. Observed and modeled BC concentrations in snow (in ng BC per g snow). The observations from the seven Arctic sites are taken from *Doherty et al.* [2010], and the observations from China (Xinjiang) are taken from *Ye et al.* [2012]. The dots show the average in the concentrations, and the bars represent the minimum and maximum concentrations. For modeled BC, the average and minimum and maximum are from the 60 year reference run with 2008 emissions with monthly mean concentrations.

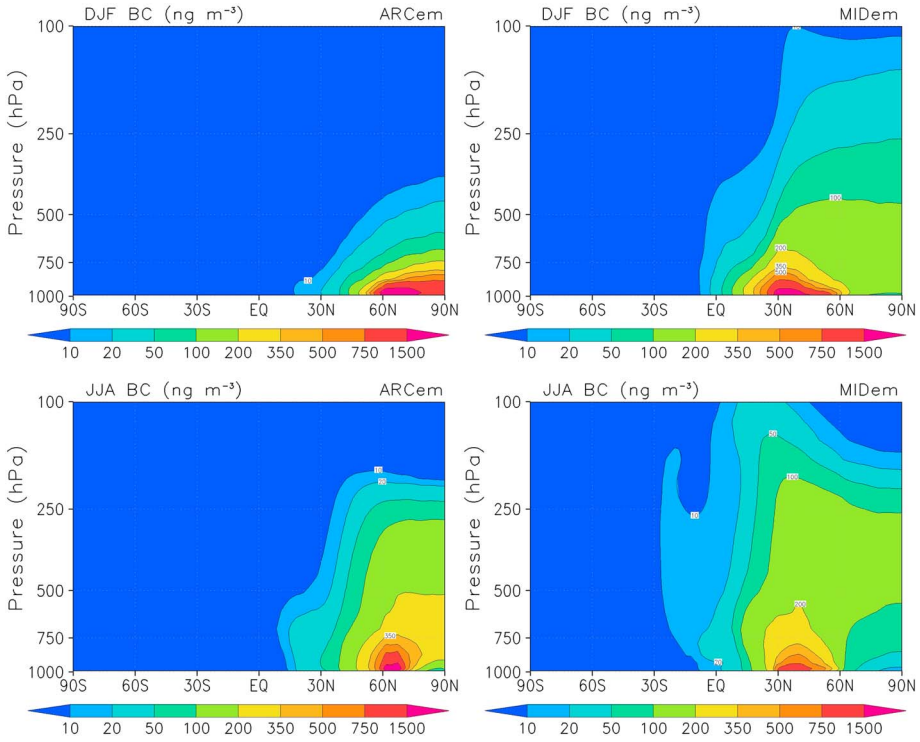

Figure 5. Difference in zonal mean BC concentrations (in ng m^{-3}) for ARCem-CTRL (left) and MIDem-CTRL (right) for the winter season Dec–Feb (top) and the summer season Jun–Aug (bottom).

[16] The zonal mean temperature responses for the two experiments for the winter, spring, and summer seasons are shown in Figure 8. In the summer season, there is a maximum warming in the free troposphere, reflecting the increased vertical mixing of BC due to convection during summer. In MIDem, the largest temperature increase is at altitudes between 500 and 200 hPa. For ARCem, the largest increase is from the surface and up to 400 hPa. For ARCem, there is also an Arctic surface warming during winter and spring. Figure 9 shows the seasonal cycle in the Arctic mean surface temperature change for the two experiments. ARCem has a larger surface temperature response in all months, with a maximum during late autumn/winter. The increase in surface temperatures during winter, when the radiative forcing of BC is very small, may be linked to a dynamical response in the sea ice and/or changes in cloudiness. Figure 10 shows the monthly mean response in the sea ice and snow cover. During the winter season, the sea ice reaches full recovery, and then additional BC leads to enhanced melting in spring and summer. For ARCem, the reduction in the sea ice is 20–50% during summer, reaching a maximum in September when the sea ice has its minimum extension. Model studies and observations show that reductions in sea-ice cover in autumn coincide with an increase in low clouds with enhanced evaporation from the open water [*Palm et al.*, 2010; *Vavrus et al.*, 2011]. Enhancement of low clouds during autumn and

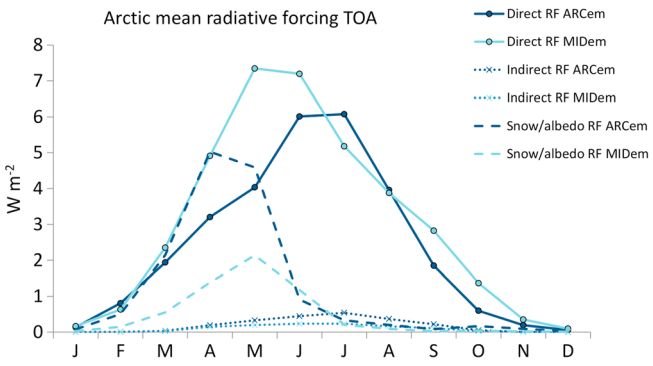

Figure 6. Arctic monthly mean (60–90°N) direct, indirect and snow/albedo (from BC on snow on land) TOA RF for ARCem-CTRL and MIDem-CTRL. Units in W m^{-2}.

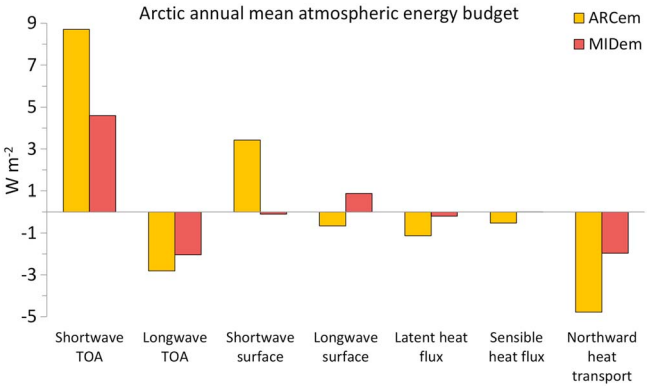

Figure 7. Change in Arctic annual mean (60–90°N) atmospheric energy budget for ARCem-CTRL (yellow) and MIDem-CTRL (red). The northward heat transport is calculated as a residual of the TOA and surface energy budget. All TOA (surface) energy budget terms are defined positive when the atmosphere (surface) gains energy. Units in W m^{-2}.

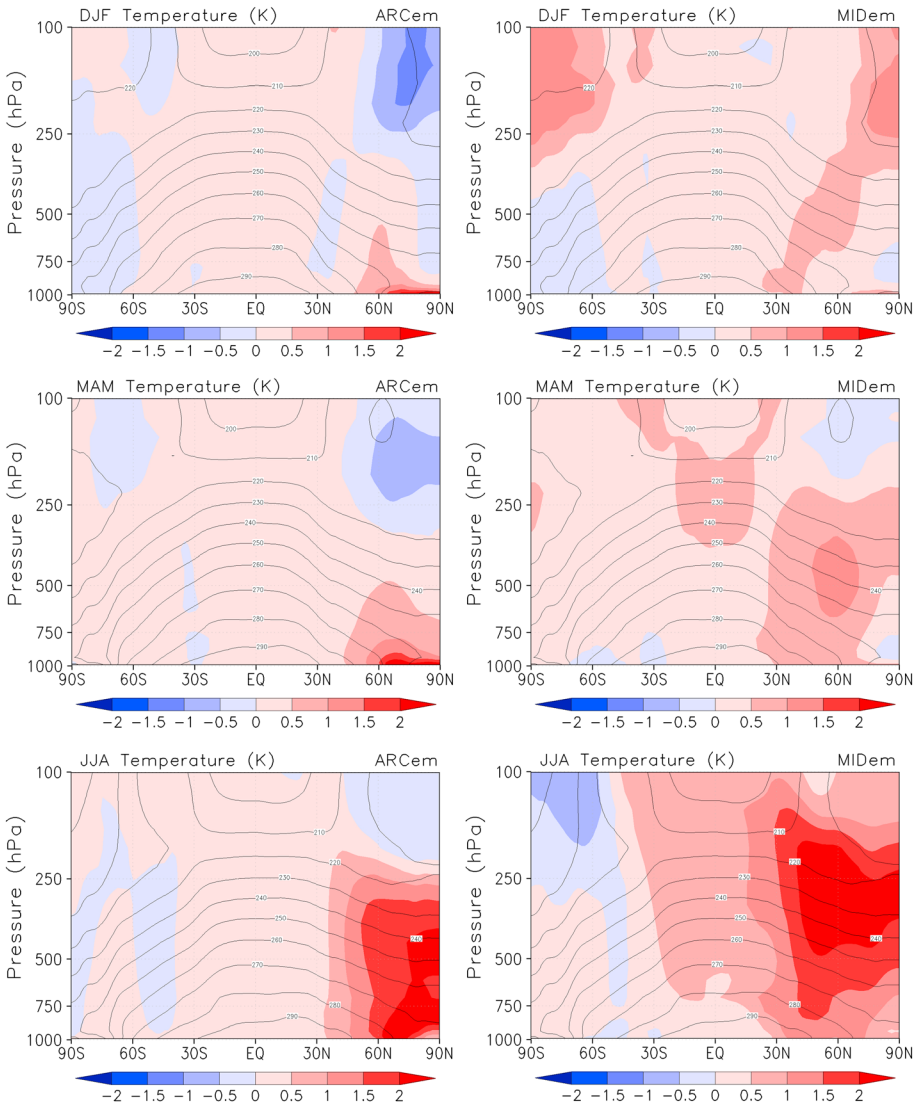

Figure 8. Change in the zonal mean temperature (in K) for ARCem-CTRL (left) and MIDem-CTRL (right) for the winter season Dec–Feb (top), spring Mar–May (middle), and the summer season Jun–Aug (bottom). The contour lines show the zonal mean temperature in the reference run (CTRL).

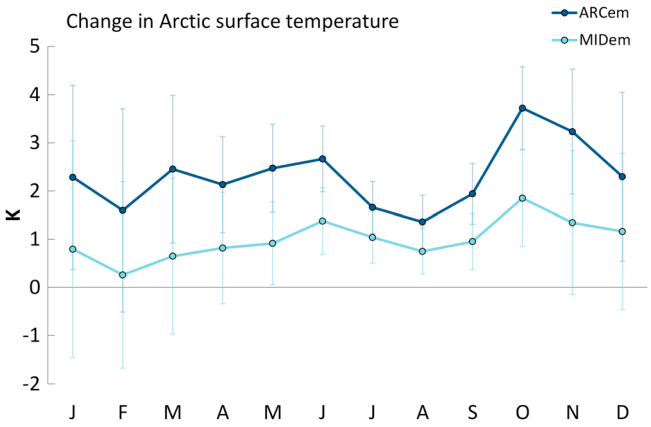

Figure 9. Change in Arctic monthly mean (60–90°N) surface temperature (in K) for ARCem-CTRL and MIDem-CTRL. Bars represent one standard deviation.

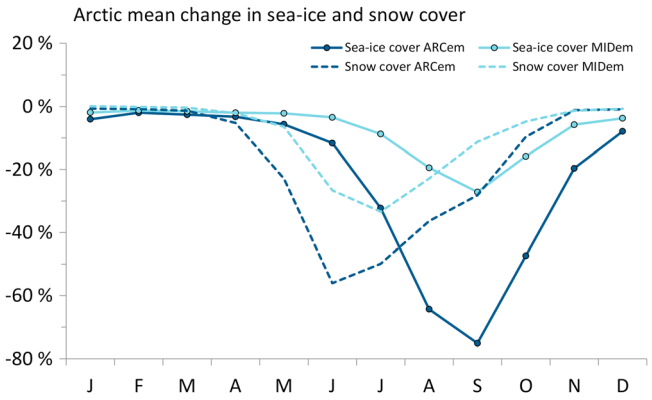

Figure 10. Change in Arctic monthly mean (60–90°N) snow cover and sea-ice cover (in % change) between ARCem-CTRL (solid line) and MIDem-CTRL (stippled line).

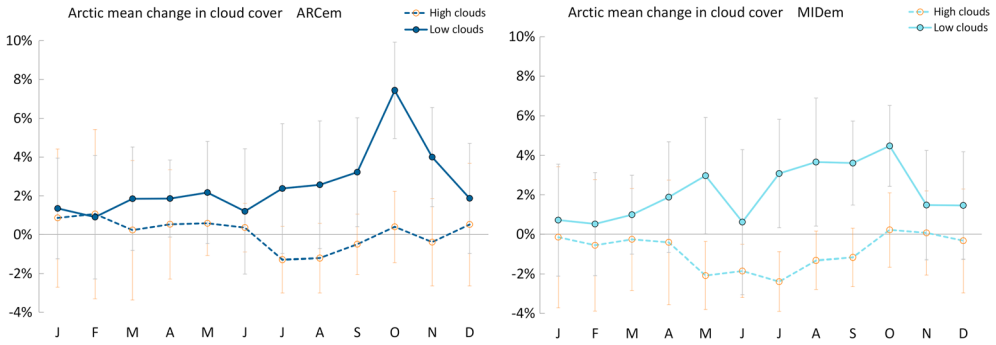

Figure 11. Change in the Arctic monthly mean (60–90°N) high and low cloud cover (in absolute change) for ARCem-CTRL (left) and MIDem-CTRL (right). The lines represent one standard deviation.

winter in the Arctic has a positive feedback on the surface temperatures (and sea-ice loss) as the clouds trap outgoing longwave radiation and reemit some of it back to the surface.

[17] Figure 11 shows the change in cloud cover for high and low clouds. In MIDem, where most of the Arctic BC is located at higher altitudes, there is a decrease in high clouds during summer and an increase in the low clouds. The increase in low clouds is followed by an increase in the downwelling longwave radiation. The increase in low clouds and downwelling longwave radiation is also apparent in ARCem, especially during the late autumn/winter season. The only significant change in clouds within 2 standard

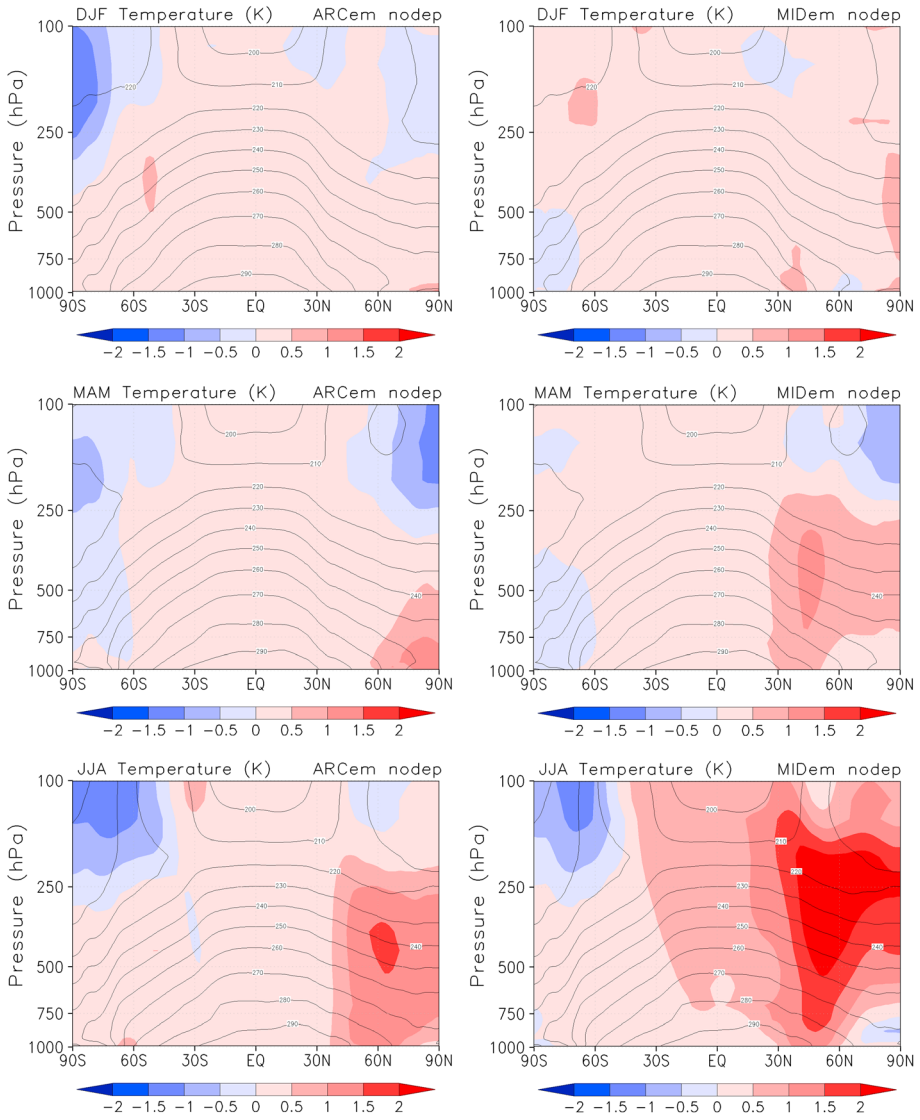

Figure 12. As in Figure 8, but for the experiments without deposition of BC.

deviations is the increase in low clouds during October. The decrease in the high clouds during summer in MIDem, where most of the BC is located in the free troposphere, may be due to a semidirect effect of BC, where the enhanced temperatures evaporate the clouds. However, since we are not applying a feedback analysis in this study, we cannot distinguish whether the changes in cloudiness are caused by a semidirect effect of BC, or to increased temperatures and/or decreased sea-ice cover. In fact, by looking at the first few months of the model run, there is no significant signal in the cloud response, indicating that the slower sea-ice feedback dominates over the fast cloud response. Similar to many other climate models, NorESM overestimates the liquid water content in Arctic clouds during winter, making the clouds too optically thick [*de Boer et al*., 2011; *Kay et al*., 2012]. This may underestimate the indirect effect of BC.

[18] The Arctic annual mean surface temperature response for ARCem is 2.3 K and 0.99 K for MIDem. When the ARCem experiment is run without the climate effect of BC deposition on snow and sea ice, the temperature increase reduces to 0.74 K. Thus, emissions within the Arctic over two thirds of the surface temperature response can be attributed to the darkening of snow and sea ice and associated feedbacks. The reduction in sea-ice cover is significantly less for the ARCem without deposition of BC. The zonal mean temperature response for the experiments without BC deposition is shown in Figure 12. The difference in the temperature response when BC deposition is included, and when it is not, is confined to the surface layer.

[19] The main goal of this study is to estimate the Arctic surface temperature increase in response to increased emissions of BC. Comparing the Arctic RF per unit (global mean) emitted mass for the two different emission regions, we find that ARCem has over a factor two higher forcing per unit emission than MIDem (0.38 vs. 0.17 Wm^{-2} per Tg BC yr^{-1}). The Arctic temperature response per unit emission, however, is almost five times as large for ARCem as for MIDem (0.24 vs. 0.05 K per Tg BC yr^{-1}). According to the results from these simulations, emitting BC north of 60°N will therefore almost give a factor five increase of the surface temperature response in the Arctic compared to emitting the same amount of BC at midlatitudes.

[20] The ARCem experiment is based on present-day emissions in the Arctic associated with large uncertainties [*Stohl et al*., 2013], and the results could be sensitive to the geographical distribution of the emissions (dominated by flaring in Russia). Thus, we have performed an additional coupled experiment emitting a fixed amount of BC in every grid cell north of 60°N ("gridARC"). The experiment has the same forcing per unit emission as ARCem: 0.37 Wm^{-2} per Tg BC yr^{-1}. The Arctic surface temperature change per unit emission in this experiment is 0.38 K per Tg BC yr^{-1} compared to 0.24 K per Tg yr^{-1} for ARCem. The response is slightly higher, but comparable to ARCem, even if the distribution of the emissions is different. This suggests that to first order the response we get in the Arctic can be generalized for future emissions within Arctic.

4. Discussion

[21] In this study, we focus on impacts on Arctic climate from BC emissions in midlatitudes or within the Arctic. Previous studies of Arctic climate response to BC have a somewhat different perspective in that emission are driving the perturbations, but rather perturbation of regional concentration profiles [*Shindell and Faluvegi*, 2009; *Flanner*, 2013; *Sand et al*., 2013]. When the BC aerosols are emitted in the lowest model layer within the Arctic, they tend to remain at lower altitudes and are more easily deposited at the surface. This causes an enhanced Arctic surface warming compared to emissions at lower latitudes. *Flanner* [2013] found similar results for prescribed Arctic BC in the lowest atmospheric layer, while BC perturbations at higher altitudes gave surface cooling. Note that an earlier study showed the same behavior exists for BC perturbations at the global scale [*Ban-Weiss et al*., 2012]. *Shindell and Faluvegi* [2009] and *Sand et al*., [2013] perturbed the distribution of present-day BC from all global sources, keeping the relative vertical profile unchanged. Both studies found a surface cooling for BC in the Arctic atmosphere (neglecting the snow/albedo effect) due to a reduction in both the meridional heat transport and the downward solar radiation at the surface. For present-day Arctic BC, most of the climate models seem to overestimate the concentrations in the free troposphere and underestimate the concentrations near the surface, our model included [*Koch et al*., 2009b]. Such a vertical distribution might underestimate the climate efficacy and the surface warming by BC in the Arctic.

[22] For ARCem, the RF of the snow/albedo reduction is about half of the TOA atmospheric direct effect, while the surface temperature response is to a large extent attributed to increased absorption by BC on snow and sea ice and decreased surface albedo. Even though the model is in good agreement with the observed BC concentrations in snow (Figure 4), one should, however, be careful to conclude, since the relative distribution of BC in the atmosphere and surface is governed by highly uncertain model boundary layer processes. For example, there are indications that NorESM may have a too stable or thin Arctic boundary layer and/or too high convective transport globally which influence the vertical distribution of BC. While NorESM underestimates surface BC concentrations, it is among the models with the highest BC concentrations in the free troposphere [*Samset et al*., 2013]. This indicates that the convective transport in NorESM may be too strong. In the midlatitudes, the convective transport can redistribute the aerosols away from the source areas. Episodes of large-scale blocking events in the Northern hemisphere during winter are a frequent transport source of pollutants from northern Eurasia into the Arctic [*Iversen and Joranger*, 1985; *Stohl*, 2006]. The lack of blocking events, possibly related to the relative coarse resolution of the model, may underestimate the meridional transport toward the Arctic [*Iversen et al*., 2013]. To what extent this influence the perturbations that are analysed here is difficult to quantify.

[23] In order to get a significant signal in the highly variable Arctic climate, we had to scale up the present-day emissions quite substantially. In particular for ARCem, this gave a strong response in the sea-ice cover. We assume that the climate signal we get is linear, so the response is scalable down to 1 × emissions, but we cannot rule out the possibility of nonlinear effects in the climate system.

[24] We have run a coupled earth system model for 60 model years which is not sufficient to reach an equilibrium

state in the ocean model. The final climate response will therefore likely be even larger than reported in this study.

[25] Sources that emit BC also emit a variety of other gases and/or particles that may either warm or cool the climate [*Bond et al*., 2013]. Thus, the net forcing may be either positive or negative depending on the amount and chemical composition of the co-emitted species. The main emitted species that can change the sign of the net forcing are particulate OM and sulfur dioxide. In the Arctic, reflective species like sulfur dioxide may not have a large impact on the albedo effect. Some emission sources, e.g., diesel engines or flaring, have a higher amount of BC relative to the co-emitted species, while emissions from open burning and shipping have a higher amount of co-emitted species. In order to make mitigation actions for different emissions activities, the actual climate change will depend on the effect of all the co-emitted species. This issue is not treated in this study. A step further on this study would be to investigate different sectors emitting BC, and to include the effect of the co-emitted species in the different sectors.

5. Concluding Remarks

[26] Using a coupled climate model we find that the Arctic climate has a significantly larger sensitivity (per unit emitted mass) to BC emitted within the Arctic compared to BC emitted at midlatitudes. Emitting BC in the Arctic will almost give a fivefold increase in the Arctic surface temperature response compared to emitting the same amount of BC at midlatitudes. A large fraction of the emitted BC within the Arctic stays in the lowermost layers in the atmosphere and gets deposited at the surface. The increased absorption of BC deposited on snow and the associated feedbacks in snow cover, sea ice, and clouds in the Arctic explain two thirds of the surface temperature increase.

[27] Since most of the present-day BC is emitted at midlatitudes, in total the emissions from midlatitudes has the largest impact on the Arctic climate, despite the fact that the BC transported into the Arctic has a small or negative impact on the surface temperatures (neglecting the impact of surface deposition) [*Shindell and Faluvegi*, 2009; *Sand et al*., 2013]. Today, emissions of BC in the Arctic are low. However, since the surface temperature response per unit emission is almost five times larger for BC emitted in the Arctic compared to midlatitudes, even a small increase in the emissions would have a large climate impact. Changes in the Arctic climate influence the global climate, and there is a great need for improving cleaner technologies if further development is to take place within the Arctic.

[28] **Acknowledgments.** We would like to thank three anonymous reviewers for useful comments. This study was funded by the Norwegian Research Council through the Earthclim project and the Programme for supercomputing (NOTUR) through a grant for computing time. We acknowledge the CRAICC project. We would also like to thank NCAR and NCAR staff for early access to model code for CCSM/CESM.

References

AMAP (2011). The impact of black carbon on Arctic climate. *AMAP Technical Report No. 4* (2011), Arctic Monitoring and Assessment Programme (AMAP), Oslo, Norway.

AMAP (2012), Snow, Water, Ice and Permafrost in the Arctic (SWIPA) 2011, Arctic Monitoring and Assessment Programme (AMAP), Oslo, Norway.

Ban-Weiss, G., L. Cao, G. Bala, and K. Caldeira (2012), Dependence of climate forcing and response on the altitude of black carbon aerosols, *Clim. Dynam.*, *38*(5-6), 897–911, doi:10.1007/s00382-011-1052-y.

Bentsen, M., et al. (2013), The Norwegian Earth System Model, NorESM1-M – Part 1: Description and basic evaluation of the physical climate, *Geosci. Model Dev.*, *6*(3), 687–720, doi:10.5194/gmd-6-687-2013.

de Boer, G., W. Chapman, J. E. Kay, B. Medeiros, M. D. Shupe, S. Vavrus, and J. Walsh (2011), A characterization of the present-day Arctic atmosphere in CCSM4, *J. Climate*, *25*(8), 2,676–2,695, doi:10.1175/JCLI-D-11-00228.1.

Bond, T. C., et al. (2013), Bounding the role of black carbon in the climate system: A scientific assessment, *J. Geophys. Res. Atmos.*, *118*, 1–173, doi:10.1002/jgrd.50171.

Corbett, J. J., D. A. Lack, J. J. Winebrake, S. Harder, J. A. Silberman, and M. Gold (2010), Arctic shipping emissions inventories and future scenarios, *Atmos. Chem. Phys.*, *10*(19), 9,689–9,704, doi:10.5194/acp-10-9689-2010.

Doherty, S. J., S. G. Warren, T. C. Grenfell, A. D. Clarke, and R. E. Brandt (2010), Light-absorbing impurities in Arctic snow, *Atmos. Chem. Phys.*, *10*(23), 11,647–11,680, doi:10.5194/acp-10-11647-2010.

Flanner, M. G. (2013), Arctic climate sensitivity to local black carbon, *J. Geophys. Res. Atmos.*, *118*, 1–12, doi:10.1002/jgrd.50176.

Flanner, M. G., and C. S. Zender (2005), Snowpack radiative heating: Influence on Tibetan Plateau climate, *Geophys. Res. Lett.*, *32*, L06501, doi:10.1029/2004GL022076.

Flanner, M. G., C. S. Zender, J. T. Randerson, and P. J. Rasch (2007), Present day climate forcing and response from black carbon in snow, *J. Geophys. Res.*, *112*, D11202, doi:10.1029/2006JD008003.

Flanner, M. G., C. S. Zender, P. G. Hess, N. M. Mahowald, T. H. Painter, V. Ramanathan, and P. J. Rasch (2009), Springtime warming and reduced snow cover from carbonaceous particles, *Atmos. Chem. Phys.*, *9*(7), 2,481–2,497, doi:10.5194/acp-9-2481-2009.

Gent, P. R., et al. (2011), The Community Climate System Model Version 4, *J. Climate*, *24*(19), 4,973–4,991, doi:10.1175/2011JCLI4083.1.

Hansen, J., and L. Nazarenko (2004), Soot climate forcing via snow and ice albedos, *P. Natl. Acad. Sci. USA*, *101*(2), 423–428, doi:10.1073/pnas.2237157100.

Hansen, J., M. Sato, R. Ruedy, A. Lacis, and V. Oinas (2000), Global warming in the twenty-first century: An alternative scenario, *P. Natl. Acad. Sci. USA*, *97*(18), 9,875–9,880, doi:10.1073/pnas.170278997.

Hansen, J., et al. (2005), Efficacy of climate forcings, *J. Geophys. Res.*, *110*, D18104, doi:10.1029/2005JD005776.

Hunke, E. C., and W. H. Lipscomb (2008), CICE: The Los Alamos Sea Ice Model, documentation and software, version 4.0, Tech. Rep. LACC-06-012, Los Alamos National Laboratory, Los Alamos, New Mexico, USA.

Intergovernmental Panel on Climate Change (2007), *Climate Change 2007: The Physical Science Basis. Contribution of Working Group I to the Fourth Assessment Report of the Intergovernmental Panel on Climate Change*, Cambridge Univ. Press, Cambridge, U. K.

Iversen, T., and E. Joranger (1985), Arctic air pollution and large scale atmospheric flows, *Atmos. Environ.*, *19*(12), 2,099–2,108, doi:10.1016/0004-6981(85)90117-9.

Iversen, T., et al. (2013), The Norwegian Earth System Model, NorESM1-M -Part 2: Climate response and scenario projections, *Geosci. Model Dev.*, *6*(2), 389–415, doi:10.5194/gmd-6-389-2013.

Jacobson, M. Z. (2004), Climate response of fossil fuel and biofuel soot, accounting for soot's feedback to snow and sea ice albedo and emissivity, *J. Geophys. Res.*, *109*, D21201, doi:10.1029/2004JD004945.

Jacobson, M. Z. (2010), Short-term effects of controlling fossil-fuel soot, biofuel soot and gases, and methane on climate, Arctic ice, and air pollution health, *J. Geophys. Res.*, *115*, D14209, doi:10.1029/2009JD013795.

Jacobson, M. Z., J. Wilkerson, S. Balasubramanian, W. Jr.Cooper, and N. Mohleji (2012), The effects of rerouting aircraft around the arctic circle on arctic and global climate, *Clim. Change*, *115*(3-4), 709–724, doi:10.1007/s10584-012-0462-0.

Kay, J. E., et al. (2012), Exposing global cloud biases in the Community Atmosphere Model (CAM) Using satellite observations and their corresponding instrument simulators, *J. Climate*, *25*(15), 5,190–5,207, doi:10.1175/JCLI-D-11-00469.1.

Kirkevåg, A., et al. (2013), Aerosol–climate interactions in the Norwegian Earth System Model – NorESM1-M, *Geosci. Model Dev.*, *6*(1), 207–244, doi:10.5194/gmd-6-207-2013.

Klimont, Z., et al. (2009), Projections of SO2, NOx and carbonaceous aerosols emissions in Asia, *Tellus B*, *61*(4), 602–617, doi:10.1111/j.1600-0889.2009.00428.x.

Klimont, Z., K. Kupiainen, C. Heyes, P. Purohit, J. Cofala, P. Rafaj, and W. Schoepp (2013), Global anthropogenic emissions of particulate matter, paper in preparation.

Klonecki, A., P. Hess, L. Emmons, L. Smith, J. Orlando, and D. Blake (2003), Seasonal changes in the transport of pollutants into the Arctic troposphere-model study, *J. Geophys. Res.*, *108*(D4), 8367, doi:10.1029/2002JD002199.

Koch, D., and J. Hansen (2005), Distant origins of Arctic black carbon: A Goddard Institute for Space Studies ModelE experiment, *J. Geophys. Res.*, *110*, D04204, doi:10.1029/2004JD005296.

Koch, D., S. Menon, A. Del Genio, R. Ruedy, I. Alienov, and G. A. Schmidt (2009a), Distinguishing aerosol impacts on climate over the past century, *J. Climate*, *22*(10), 2,659–2,677, doi:10.1175/2008JCLI2573.1.

Koch, D., et al. (2009b), Evaluation of black carbon estimations in global aerosol models, *Atmos. Chem. Phys.*, *9*(22), 9,001–9,026, doi:10.5194/acp-9-9001-2009.

Koch, D., et al. (2011a), Coupled aerosol-chemistry–climate twentieth-century transient model investigation: Trends in short-lived species and climate responses, *J. Climate*, *24*(11), 2,693–2,714, doi:10.1175/2011JCLI3582.1.

Koch, D., et al. (2011b), Soot microphysical effects on liquid clouds, a multi-model investigation, *Atmos. Chem. Phys*, *11*, 1,051–1,064, doi:10.5194/acp-11-1051-2011.

Kristjánsson, J. E. (2002), Studies of the aerosol indirect effect from sulfate and black carbon aerosols, *J. Geophys. Res.*, *107*(D15), 4246, doi:10.1029/2001JD000887.

Kupiainen, K., and Z. Klimont (2007), Primary emissions of fine carbonaceous particles in Europe, *Atmos. Environ.*, *41*(10), 2,156–2,170, doi:10.1016/j.atmosenv.2006.10.066.

Lamarque, J., et al. (2010), Historical (1850–2000) gridded anthropogenic and biomass burning emissions of reactive gases and aerosols: Methodology and application, *Atmos. Chem. Phys.*, *10*, 7,017–7,039, doi:10.5194/acp-10-7017-2010.

Law, K. S., and A. Stohl (2007), Arctic air pollution: Origins and impacts, *Science*, *315*(5818), 1,537–1,540, doi:10.1126/science.1137695.

Neale, R. B., et al. (2010), Description of the NCAR Community Atmosphere Model (CAM 4.0), NCAR Technical Note.

Ødemark, K., S. Dalsøren, B. Samset, T. Berntsen, J. Fuglestvedt, and G. Myhre (2012), Short-lived climate forcers from current shipping and petroleum activities in the Arctic, *Atmos. Chem. Phys.*, *12*, 1,979–1,993, doi:10.5194/acp-12-1979-2012.

Palm, S. P., S. T. Strey, J. Spinhirne, and T. Markus (2010), Influence of Arctic sea ice extent on polar cloud fraction and vertical structure and implications for regional climate, *J. Geophys. Res.*, *115*, D21209, doi:10.1029/2010JD013900.

Peters, G. P., T. B. Nilssen, L. Lindholt, M. S. Eide, S. Glomsrød, L. I. Eide, and J. S. Fuglestvedt (2011), Future emissions from shipping and petroleum activities in the Arctic, *Atmos. Chem. Phys.*, *11*(11), 5,305–5,320, doi:10.5194/acp-11-5305-2011.

Quinn, P. K., et al. (2008), Short-lived pollutants in the Arctic: Their climate impact and possible mitigation strategies, *Atmos. Chem. Phys.*, *8*(6), 1,723–1,735, doi:10.5194/acp-8-1723-2008.

Samset, B. H., et al. (2013), Black carbon vertical profiles strongly affect its radiative forcing uncertainty, *Atmos. Chem. Phys.*, *13*(5), 2,423–2,434, doi:10.5194/acp-13-2423-2013.

Sand, M., T. K. Berntsen, J. E. Kay, J. F. Lamarque, Ø. Seland, and A. Kirkevåg (2013), The Arctic response to remote and local forcing of black carbon, *Atmos. Chem. Phys.*, *13*(1), 211–224, doi:10.5194/acp-13-211-2013.

Shindell, D. (2007), Local and remote contributions to Arctic warming, *Geophys. Res. Lett.*, *34*, L14704, doi:10.1029/2007GL030221.

Shindell, D., and G. Faluvegi (2009), Climate response to regional radiative forcing during the twentieth century, *Nat. Geosci.*, *2*(4), 294–300, doi:10.1038/ngeo473.

Shindell, D., et al. (2012), Simultaneously mitigating near-term climate change and improving human health and food security, *Science*, *335*(6065), 183–189, doi:10.1126/science.1210026.

Stohl, A. (2006), Characteristics of atmospheric transport into the Arctic troposphere, *J. Geophys. Res.*, *111*, D11306, doi: 10.1029/2005JD006888.

Stohl, A., Z. Klimont, S. Eckhardt, and K. Kupiainen (2013), Why models struggle to capture Arctic Haze: The underestimated role of gas flaring and domestic combustion emissions, *Atmos. Chem. Phys. Discuss.*, *13*(4), 9,567–9,613, doi:10.5194/acpd-13-9567-2013.

Storelvmo, T., J. E. Kristjánsson, S. J. Ghan, A. Kirkevåg, Ø. Seland, and T. Iversen (2006), Predicting cloud droplet number concentration in Community Atmosphere Model (CAM)-Oslo, *J. Geophys. Res.*, *111*, D24208, doi:10.1029/2005JD006300.

Vavrus, S., M. Holland, and D. Bailey (2011), Changes in Arctic clouds during intervals of rapid sea ice loss, *Clim. Dynam.*, *36*(7-8), 1,475–1,489, doi:10.1007/s00382-010-0816-0.

Ye, H., R. Zhang, J. Shi, J. Huang, S. G. Warren, and Q. Fu (2012), Black carbon in seasonal snow across northern Xinjiang in northwestern China, *Environ. Res. Lett.*, *7*(4), 044002, doi:10.1088/1748-9326/7/4/044002.